Conformational Coupling between the Cytoplasmic Carboxylic Acid and the Retinal in a Fungal Light-Driven Proton Pump†

Yuji Furutani,‡,§ Masayo Sumii,‡ Ying Fan,|| Lichi Shi,|| Stephen A. Waschuk,|| Leonid S. Brown,*,|| and Hideki Kandori*,‡,§

Department of Materials Science and Engineering, Nagoya Institute of Technology, Showa-ku, Nagoya 466-8555, Japan, Core Research for Evolutional Science and Technology (CREST), Japan Science and Technology Corporation, Kyoto 606-8502, Japan, and Department of Physics, University of Guelph, Guelph, Ontario N1G 2W1, Canada

Received September 7, 2006; Revised Manuscript Received October 4, 2006

ABSTRACT: Many fungal rhodopsins, eukaryotic structural homologues of the archaeal light-driven proton pump bacteriorhodopsin, have been discovered in the course of genome sequencing projects. Recently, two fungal rhodopsins were characterized in vitro and exhibited very different photochemical behavior. *Neurospora* rhodopsin possesses a slow photocycle and shows no ion transport, reminiscent of sensory rhodopsins, while *Leptosphaeria* rhodopsin has a fast bacteriorhodopsin-like photocycle and pumps protons light-dependently. Such a dramatic difference is surprising considering the very high degree of sequence homology of the two proteins. In this paper, we investigate whether the chemical structure of a cytoplasmic carboxylic acid, the homologue of Asp-96 of bacteriorhodopsin serving as a proton donor for the retinal Schiff base, can define the photochemical properties of fungal rhodopsins. We studied mutants of *Leptosphaeria* rhodopsin in which this aspartic acid was replaced with Glu or Asn using spectroscopy in the infrared and visible ranges. We show that Glu at this position is inefficient as a proton donor similar to a nonprotonatable Asn. Moreover, this replacement induces long-range structural perturbations of the retinal environment, as evidenced by changes in the vibrational bands of retinal (especially, hydrogen-out-of-plane modes) and neighboring aspartic acids and water molecules. The conformational coupling of the mutation site to the retinal may be mediated by helical rearrangements as suggested by the changes in amide and proline vibrational bands. We conclude that the difference in the photochemical behavior of fungal rhodopsins from *Leptosphaeria* and *Neurospora* may be ascribed, to some extent, to the replacement of the cytoplasmic proton donor Asp with Glu.

Fungal rhodopsins make up a recently discovered growing family of retinal-binding proteins classified as type I (microbial) rhodopsins (*1*−*3*). These proteins are highly homologous to the halobacterial light-driven proton pump bacteriorhodopsin (BR),[1] conserving most of the intramembrane residues that are important for proton transport (*4*−*6*), which suggests their possible ion transporting role. Because some of the homologous haloarchaeal rhodopsins perform photosensory functions (*4*), and taking into account the heterotrophic nature of fungi, we find a sensory function for fungal rhodopsins may be possible as well. Several genetic studies failed to detect any serious defects in the rhodopsin knockout phenotypes of the hosts (*7*−*9*), so the physiological role of rhodopsins from Ascomycetes and Basidiomycetes remains unknown. It should be noted that in one species of Chytridiomycetes a rhodopsin was suggested to mediate a phototaxis of zoospores (*10*), but the gene has not been cloned so far.

In the absence of the physiological data, biophysical studies on heterologously expressed fungal rhodopsins provided interesting and suggestive information about their putative functions. The first heterologously expressed rhodopsin from *Neurospora* (NR) (*7*) behaves more like a photosensory rhodopsin rather than a BR-like proton pump, contrary to the expectations based on its sequence being highly similar to that of BR (*11*, *12*). Its photocycle is slow, which is atypical for ion pumps (*4*), and the replacement of the cytoplasmic Glu-142 (the homologue of the proton donor of the Schiff base, Asp-96 in BR) with Gln does not affect the rate of the Schiff base reprotonation (*12*). Further studies suggested that the structure of the hydrogen-bonded network around the retinal Schiff base is very different between NR and BR (*13*), which may be responsible for the lack of the reprotonation switch (the Schiff base reorientation in the cytoplasmic direction) in NR. In particular, it was shown that there is no photoisomerization-induced perturbation of a strongly hydrogen bonded water molecule near the Schiff

† This work was supported in part by grants from Japanese Ministry of Education, Culture, Sports, Science, and Technology to H.K. and by the NSERC, PREA, and Research Corporation grants to L.S.B. L.S.B. acknowledges JSPS for the Invitation Fellowship, which was instrumental in the writing of this paper.

* To whom correspondence should be addressed. Phone and fax: 81-52-735-5207. E-mail: kandori@nitech.ac.jp or leonid-@physics.uoguelph.ca.

‡ Nagoya Institute of Technology.

§ CREST.

|| University of Guelph.

[1] Abbreviations: LR, *Leptosphaeria* rhodopsin; BR, bacteriorhodopsin; NR, *Neurospora* rhodopsin; *p*pR, *pharaonis* phoborhodopsin; LR_K, K intermediate of LR; NR_K, K intermediate of NR; HOOP, hydrogen-out-of-plane vibration; DMPC, 1,2-dimyristoyl-*sn*-glycero-3-phosphocholine; DMPA, 1,2-dimyristoyl-*sn*-glycero-3-phosphate.

10.1021/bi061864l CCC: $33.50
Published on Web 12/01/2006

base of NR (*13*), the feature known to correlate with the proton pumping ability in many rhodopsins (*14*). The exact structural cause of such unexpected photochemical behavior remained unknown despite the existence of some suggestive differences in the sequences of BR and NR.

The second fungal rhodopsin characterized biophysically was found in the genome of *Leptosphaeria maculans* (*5*). The sequence of *Leptosphaeria* rhodopsin (LR) was even more similar to that of BR, suggesting that it may be a proton pump. Indeed, when expressed in *Pichia pastoris*, this protein exhibited a very fast photocycle with many BR-like features and pumped protons light-dependently upon reconstitution into liposomes (*15*). The replacement of Asp-150, the homologue of Asp-96 in BR, with Asn resulted in a dramatic deceleration of the reprotonation of the Schiff base, in accord with the BR-like mechanism of proton transport. These findings established LR as the first eukaryotic retinal-based light-driven proton pump; albeit, its exact physiological role is still mysterious. In accordance with the character of its photochemistry, the low-temperature FTIR studies showed that LR possesses a strongly bound water in the retinal Schiff base vicinity, in stark contrast to NR, but exactly as expected from a proton-pumping rhodopsin (*16*). Such a large difference in the photochemistry and ion pumping ability between the proteins as structurally close as LR and NR is very surprising.

The differences in the primary structures of LR and NR have been analyzed previously (*1*, *5*, *16*). There are just two outstanding differences in the conserved residues important for the functioning of BR, one in the homologues of Glu-194 and the other in the homologues of Asp-96. The carboxylic side chain of Glu-194, known to be important for proton release in BR (*17*), is missing in NR but present as Asp-248 in LR. While the Schiff base proton donor of BR (Asp-96) is conserved as Asp-150 in LR, it is conservatively replaced in NR, being present as Glu-142 (see Figure 1 in ref *16*). It is hard to imagine that a replacement as conservative as an Asp → Glu change would abolish proton transport completely. Indeed, a glutamate residue at this position serves as a Schiff base proton donor in eubacterial proton pump proteorhodopsin (*18*), and the D96E mutant of BR was reported to be fully active in terms of proton pumping (*19*, *20*), at least in the reconstituted systems. Nevertheless, the same BR mutant in the native purple membrane exhibits very slow reprotonation of the Schiff base (*21*). Namely, the M decay time constant of the D96E mutant in aqueous suspension is 8 times larger than that of wild-type BR but 6.5 times smaller than that of the D96N mutant. It suggests that the geometry of the proton donor may be important for the optimal rate of proton translocation.

In this work, we investigated the effect of the replacement of Asp-150, the Schiff base proton donor of LR, with Glu. Our goal was to determine if this subtle sequence alteration may be responsible for the dramatic difference in the photochemical behavior of NR and LR. We found that the reprotonation of the Schiff base in LR is severely impaired when Asp-150 is replaced with Glu as much as when replaced with the nonprotonatable Asn (*15*). Moreover, we showed that the D150E mutation produces long-range effects on the protein structure and the geometry of the photoisomerized retinal, and to an extent much larger than that observed for the D150N mutant. In particular, the retinal hydrogen-out-of-plane vibrations (HOOPs) are very similar between NR and the D150E mutant of LR but different from those in wild-type LR. We conclude that the exact nature of the carboxylic residue at the position homologous to Asp-96 of BR may be important for the fast reprotonation of the Schiff base in fungal rhodopsins not only due to the differences in the proton affinity between Asp and Glu but also due to the conformational coupling of this carboxylic acid to the retinal. It is possible that the Asp → Glu substitution of the cytoplasmic proton donor is one of the key elements responsible for the functional diversification of fungal rhodopsins as represented by LR and NR.

MATERIALS AND METHODS

Expression of Leptosphaeria Rhodopsin Mutants in P. pastoris. The mutants of LR were produced by a single-step PCR from the wild-type construct and expressed in a manner analogous to that of the wild type as described below. The *L. maculans ops* gene (*5*) was modified and cloned into the pHIL-S1 vector as described previously (*15*), via a similar procedure previously used for *Neurospora* rhodopsin (*11*). The resulting protein has its N-terminus (48 residues) replaced with the yeast PHO1 signal sequence and a six-His tag added to the C-terminus (*15*). The protein was expressed in the methylotrophic yeast *P. pastoris*, strain GS115, following our optimized procedure for NR (*13*). During expression in *P. pastoris*, 5 μM all-*trans*-retinal (Sigma) was added to the growth medium approximately 24 h following induction with methanol.

Purification of the Membranes and the Protein and Reconstitution into Liposomes. Breakage of *P. pastoris* cells, isolation and solubilization of the membranes, and purification and concentration of LR were described elsewhere (*15*). *N*-Dodecyl β-D-maltoside treatment of the membranes followed by sequential centrifugations yielded a clear supernatant with membranes containing LR, suitable for optical spectroscopy, which were encased in polyacrylamide gels. The membranes suspended in deionized water (1−2 OD/mL) were treated with 0.2% DM for 5−10 min at room temperature. The gels were soaked in a buffer of the desired pH and composition for at least 2 h. For reconstitution into liposomes, Triton X-100-solubilized Ni-NTA-purified LR was added to preformed DMPC/DMPA (9:1) liposomes at a 3:1 (w/w) lipid:protein ratio. Reconstitution via detergent removal was done using Bio-Beads SM-2 (Bio-Rad). Liposomes were washed repeatedly by centrifugation at 40000*g* and frozen for further use.

Time-Resolved Spectroscopy in the Visible Range. Time-resolved laser spectroscopy in the visible range was performed on our custom-built apparatus. Photocycle excitation was provided by the second harmonic of an Nd:YAG laser (Continuum Minilite II) using ~7 ns pulses at 532 nm. Absorption changes of monochromatic light (provided by an Oriel QTH source and two monochromators) were followed using an Oriel photomultiplier with a 350 MHz wide bandwidth amplifier and a Gage AD converter (CompuScope 12100-64M). The traces were converted into a quasi-logarithmic time scale using homemade software. Global multiexponential analysis of the data was performed as described previously (*12*). For comparison, the pH dependencies of the rates of M decay for the wild type and the D150N mutant LR were taken from our earlier work (*15*).

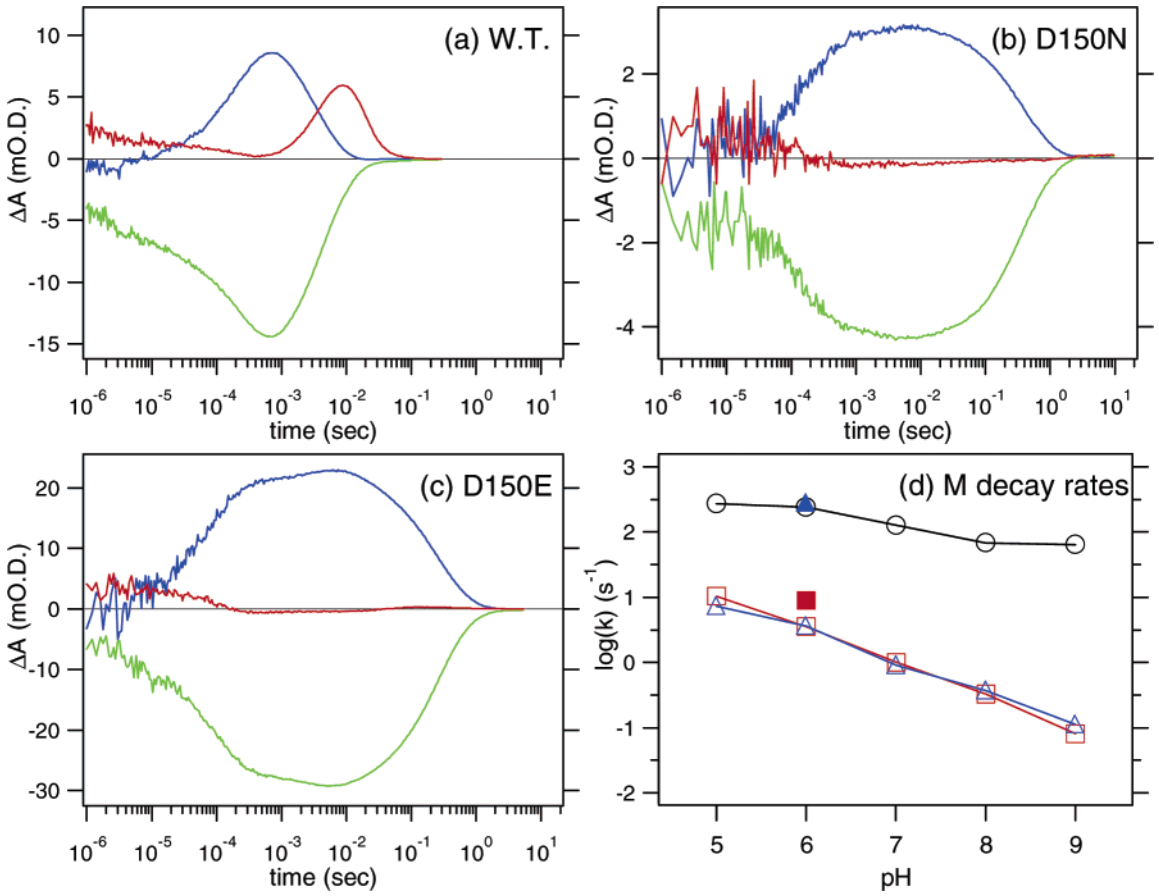

FIGURE 1: (a−c) Kinetics of light-induced absorption changes of the LR variants [wild type (a), D150N (b), and D150E (c)] in *N*-dodecyl *β*-D-maltoside-treated *P. pastoris* membranes measured at room temperature: blue for 420 nm, green for 560 nm, and red for 620 nm. The LR membranes were encased in a polyacrylamide gel and equilibrated with 0.1 M NaCl, 0.05 M MES, and 0.05 M sodium phosphate (pH 6.0). The difference in the signal amplitudes and noise levels reflects the different levels of expression. (d) pH dependence of the Schiff base reprotonation rate (the M decay at 420 nm) (the wild-type and D150N mutant curves are from ref *15*). The rates were obtained from the multiexponential analysis of the data like those of panel c but taken at varying pH or with addition of sodium azide (10 mM): black for the wild type, blue for D150N, and red for D150E. The filled symbols represent the data in the presence of azide. The conditions were the same as those for panel c, but with 0.05 M TRIS or CHES as the buffer at pH 8 or 9, respectively.

FTIR Spectroscopy. FTIR spectroscopy was performed as described previously (*22*). The LR sample reconstituted into DMPC/DMPA liposomes was washed three times with 2 mM phosphate buffer (pH 7). The pellet was resuspended in the same buffer, and the concentration was adjusted to ∼2 OD units at 535 nm/mL. An 80 μL aliquot was deposited on a BaF_2 window 18 mm in diameter and dried in a glass vessel that was evacuated with an aspirator.

The dark-adapted LR contains predominantly all-*trans*-retinal with a small proportion of 13-*cis*-retinal, but prolonged dehydration was found to increase the 13-*cis* content. For this reason, the sample was hydrated, adapted to light for 2 min at room temperature (wavelength of >450 nm), and mildly dehydrated again to be immediately rehydrated with H_2O, D_2O, or $D_2{}^{18}O$ in a controlled fashion. The sample was placed in a cell in an Oxford DN-1704 cryostat mounted in the Bio-Rad FTS-40 spectrometer. The cryostat was equipped with an Oxford ITC-4 temperature controller, and the temperature was regulated with 0.1 K precision.

Illumination with 500 nm light at 77 K for 2 min converted LR to LR_K. Since LR_K was completely reconverted to LR upon illumination with >600 nm light for 1 min, as evidenced by the spectral shape which is a mirror image of that for the LR to LR_K transition, cycles of alternating illumination with 500 and >600 nm light were repeated a number of times. The difference spectrum was calculated from two spectra constructed from 128 interferograms taken before and after the illumination. Several difference spectra obtained in this way were averaged to produce the LR_K minus LR spectrum. As earlier linear dichroism experiments revealed the random orientation of LR molecules in the liposome film, an IR polarizer was not used. For comparisons, the wild-type LR_K minus LR difference spectra were taken from Sumii et al. (*16*) and NR_K minus NR spectra from Furutani et al. (*13*).

RESULTS

Time-Resolved Spectroscopy in the Visible Range at Room Temperature. We used time-resolved difference spectroscopy in the visible range at room temperature to see whether the D150E mutation affects the rate of the Schiff base reprotonation in LR. Figure 1a−c compares the photocycle kinetics of wild-type LR with those of the D150N and D150E mutants at pH 6. As found previously (*15*), the wild-type kinetics is fast, being comparable to that of BR (Figure 1a), while that of the D150N mutant is much slower (Figure 1b). As expected from the inactivation of the Schiff base proton donor, the M decay (reprotonation of the Schiff base followed at 420 nm) becomes slower (∼2 orders of magnitude) and becomes the rate-limiting step in the photocycle of the

D150N mutant (Figure 1b). Interestingly, the D150E mutation produced a phenotype very similar to that of D150N, with very slow reprotonation of the Schiff base (Figure 1c) and the absence of the O intermediate (measured at 620 nm). The apparent equivalency of N150 and E150 over a wide pH range (5−9) is obvious from Figure 1d, where the rates of the Schiff base reprotonation are plotted versus pH, and both mutants demonstrate greatly delayed decay of the M intermediate. While in the D150N mutant the wild-type-like rate of the M decay can be restored by the addition of sodium azide (*15*), it is much less efficient in the reactivation of D150E (Figure 1d). This is similar to the known differences in the azide reactivity for different Asp-96 mutants of BR [efficient for D96N, but much less efficient for D96G and D96A (*23*, *24*)]. The data in Figure 1 suggest that only aspartic acid, but not glutamic acid (or asparagine), at position 150 can serve as an efficient donor of a proton to the Schiff base. This is despite the fact that Glu-150 seems to be protonated in the initial state as follows from the FTIR data (see below).

LR_K minus LR Difference Infrared Spectra of the Wild Type, D150N, and D150E in the 1800−900 cm^{-1} Region. One may expect no differences between the K spectra of the D150 mutants and the wild type, because the structural changes upon formation of the K intermediate are mostly localized near the retinal chromophore, while Asp-150, which corresponds to Asp-96 in BR, is located relatively far from the retinal. From the X-ray structure of BR, Asp-96 is located ∼10 Å from the retinal Schiff base, and the two groups have no hydrogen-bonded network between them (*25*). Both D150 mutants produce the K intermediate under the illumination conditions appropriate for the accumulation of this photoproduct in the wild type. However, it is clear that the introduction of Glu at position 150 shifts the C═O stretching vibration of amide I from 1649 to 1642 cm^{-1} in the ground state, the C−C stretch from 1197 to 1196 cm^{-1}, and the most prominent HOOP vibration from 958 to 978 cm^{-1} in the K intermediate (Figure 2). These results indicate that the ground state structure of LR is perturbed by the introduction of a Glu residue at this position and the structural changes of the retinal are affected. The D150N mutant exhibits spectral features intermediate between those of the wild type and the D150E mutant, suggesting a weaker influence of this replacement on the protein structure.

HOOP Vibrations of the Retinal Chromophore. It is well-known that distortion of the retinal chromophore after photoisomerization increases the intensity of its HOOP vibrations (*22*, *26*−*30*). In the K intermediate spectrum of wild-type LR, the most intense band is observed at 958 cm^{-1}, which is downshifted to 950 cm^{-1} upon deuteration of the Schiff base (Figure 3a). On the basis of the analogy to BR (*31*), these bands were tentatively assigned to the C15−HOOP vibration, which means that the retinal chromophore is distorted at the C15 position upon retinal isomerization in LR. In the K spectrum of NR (Figure 3d), the most intense band is observed at 983 cm^{-1}, which is at a frequency higher than those of BR and LR. A similar upshift of the C15−HOOP vibration has been reported for the K_L intermediate of BR trapped at 135 K (*32*). Recently, we assigned the HOOP vibrations of the K intermediate of *p*pR using systematically deuterated retinals and found that the C15−HOOP mode consists of multiple bands at 1001, 994, and

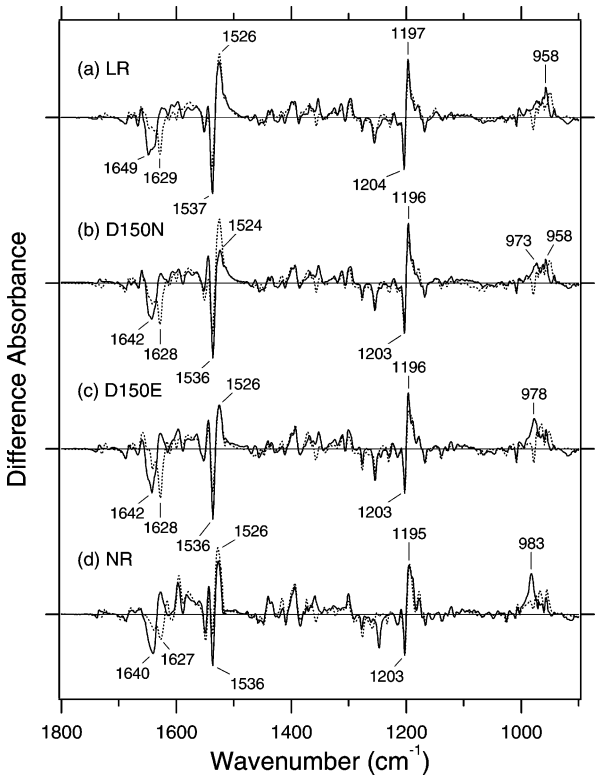

FIGURE 2: Difference infrared spectra between the K intermediates and the unphotolyzed states of wild-type (a), D150N (b), and D150E (c) LR and wild-type NR (d) in the 1800−900 cm^{-1} region. The solid and dotted lines represent the spectra of samples measured under H_2O and D_2O hydration, respectively. The spectra of D150N, D150E, and wild-type NR are normalized to that of wild-type LR according to the intensities of the C−C stretching vibration of the retinal at 1204 cm^{-1}. One division of the *y*-axis corresponds to 0.008 absorbance unit.

987 cm^{-1} (*27*). These bands have frequencies much higher than that of the K intermediate of BR and LR. Conclusive interpretation has not been achieved yet, but it is probably caused by vibrational coupling with neighboring methyl or hydrogen groups. The frequency of the C15−HOOP vibration should be determined by the structure of the retinal molecule itself, which is perturbed by the surrounding amino acid residues. Thus, it is surprising that the C15−HOOP vibration upshifts to 978 cm^{-1} in the K spectrum of the D150E mutant (Figure 3c), where the substitution site is far from the retinal. The frequency of this vibration in the D150E mutant of LR is much closer to that of NR than of wild-type LR. Interestingly, the spectral features of the D150N mutant (Figure 3b) are between those of the wild type and the D150E mutant. These results suggest that the protein structure around the Schiff base is influenced by these mutations, probably through the helix−helix interactions mediated by Thr-87 in helix B and Asp-150 in helix C (Thr-46 and Asp-96 in BR). This perturbation probably affects the thermal stability of the K intermediate and produces a K_L-like intermediate in the D150E mutant even at 77 K, because we confirmed the existence of the K_L intermediate of LR at 130 K, which has an intense C15−HOOP vibration at 981 cm^{-1} as shown below.

The negative bands at 1008, 978, and 918 cm^{-1} could be assigned to the methyl rocking, the N−D in-plane bending, and the N−HOOP and C15−HOOP coupled vibrations, respectively. These bands are not changed by the mutations,

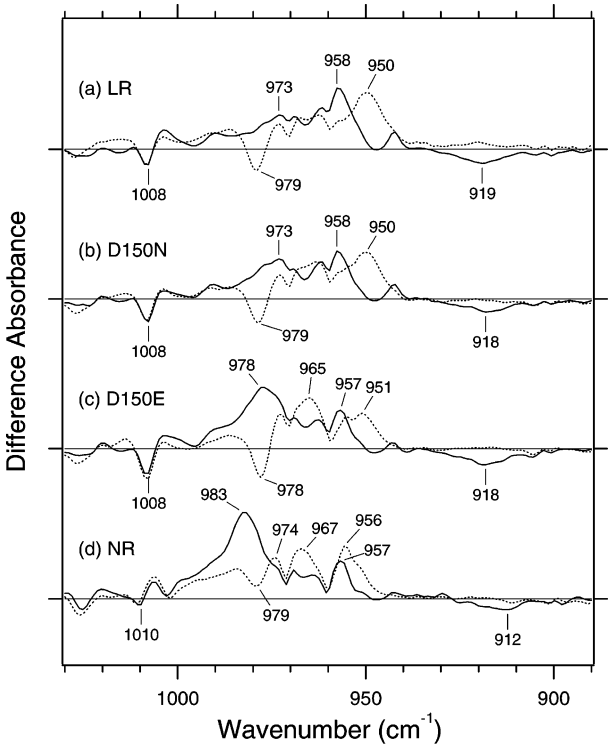

FIGURE 3: Difference infrared spectra between the K intermediates and the unphotolyzed states of wild-type (a), D150N (b), and D150E (c) LR and wild-type NR (d) in the 1030−890 cm^{-1} region, where hydrogen-out-of-plane (HOOP) vibrations of the retinal can be observed. The solid and dotted lines represent the spectra of samples measured under H_2O and D_2O hydration, respectively. One division of the *y*-axis corresponds to 0.0035 absorbance unit.

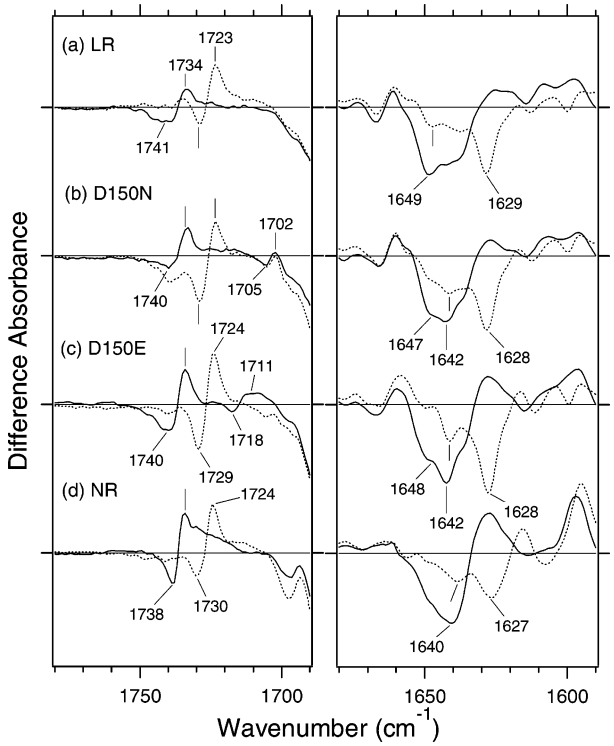

FIGURE 4: Difference infrared spectra between the K intermediates and the unphotolyzed states of wild-type (a), D150N (b), and D150E (c) LR and wild-type NR (d) in the 1780−1590 cm^{-1} region. The solid and dotted lines represent the spectra of samples measured under H_2O and D_2O hydration, respectively. One division of the *y*-axis corresponds to 0.0008 (left) and 0.004 (right) absorbance unit.

so the Schiff base itself is not perturbed in the ground state. This conclusion is also supported by the N−D stretching vibrations of the Schiff base described below.

The Protein Backbone of LR Is Perturbed by the Replacement of Asp-150 with Asn or Glu. The C═O stretches of the carboxyl and carbonyl groups and the amide I vibrations are shown in the left and the right panels of Figure 4, respectively. The data in the left panel are magnified 5 times to match the amplitudes in the right panel. The bands at 1741 (−)/1734 (+) cm^{-1} in wild-type LR and those at 1738 (−)/1734 (+) cm^{-1} in wild-type NR can be assigned to Asp-169 in LR and Asp-161 in NR, respectively, which correspond to Asp-115 in BR (*33*). This indicates that the aspartic acid at this position is protonated in both LR and NR, and the hydrogen bonding alterations upon retinal photoisomerization are similar. It should be, however, noted that the frequencies and intensities in LR are similar to those in BR (*16*) and those in NR are somewhat different (*13*). The amplitude of these bands of LR in Figure 4 is 0.000174, while that of NR (when normalized to the negative band at 1204 cm^{-1}) is 0.000375, which is ∼2 times larger. It is interesting that the relative intensities of these bands in the D150N (0.000222) and especially D150E (0.000328) mutants are larger than those of wild-type LR but similar to those of NR. The similar feature is observed in the spectra measured in D_2O as well. These results suggest that the structural changes around Asp-169 in these mutants are more similar to those of NR because of the introduction of Asn or Glu at position 150 in LR (NR has Glu at this site). Additionally, small but prominent mutation-induced bands were observed in the D150N and D150E mutants. The deuteration insensitive bands at 1705 (−)/1702 (+) cm^{-1} and the deuteration sensitive bands at 1718 (−)/1711 (+) cm^{-1} can be assigned to the carbonyl C═O stretch of Asn-150 and the protonated carboxyl C═O stretch of Glu-150 in the respective mutant proteins. This result indicates that Glu-150 is protonated in the initial state and has a potential to work as a proton donor for the Schiff base, which is surprising considering that the M decay kinetics of the D150E mutant (Figure 1c) clearly shows that the reprotonation of the Schiff base is severely impaired.

The global structural impact of the substitutions was also confirmed by the amide I bands shown in the right panel of Figure 4. The negative band at 1649 cm^{-1} in the wild-type LR appears to be downshifted to 1642 cm^{-1} in the D150N and D150E mutants. Because the same feature was observed in the spectra measured in D_2O, it does not originate from the C═N stretch of the Schiff base (even though the Schiff base C═N vibration is indeed present in this spectral region but downshifts to 1627−1629 cm^{-1} upon deuteration). The assignment is also supported by the position of the N−D stretch of the Schiff base (see below), which was not influenced by the mutations. Thus, the mutations at Asp-150 do not affect the Schiff base itself but have an effect on the backbone structure of the protein.

The D150E and D150N Mutations in LR Cause the Intensity Change of the Bands in the Frequency Region of the C−N Stretching Vibrations of Proline. In the previous FTIR experiments on BR with ^{15}N-labeled prolines, the bands at 1454 (+)/1435 (−) and 1417 (+)/1400 (−) cm^{-1} in the K minus BR spectra were assigned to C−N proline vibrations (*34*). Three proline residues in the membrane region, Pro-50 on helix B, Pro-91 on helix C, and Pro-186 on helix F,

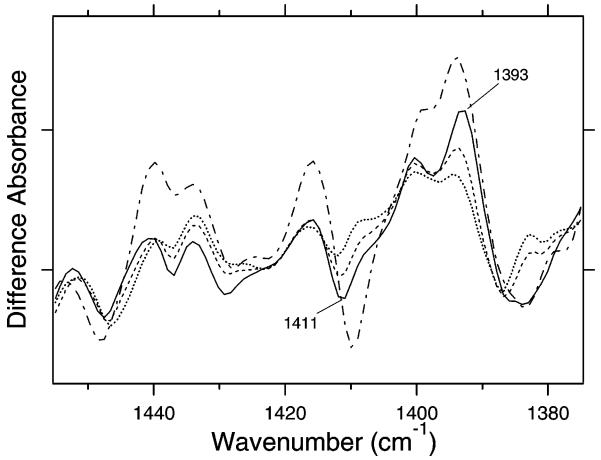

FIGURE 5: Difference infrared spectra between the K intermediates and the unphotolyzed states in the 1455−1375 cm^{-1} region measured under D_2O hydration. The spectra of wild-type (···), D150N (- - -), and D150E (—) LR and wild-type NR (—·—) are compared. One division of the *y*-axis corresponds to 0.001 absorbance unit.

were considered to be candidates for these vibrational bands. In Figure 5, we show that in the same spectral region in LR the intensities of the bands at 1393 (+)/1411 (−) cm^{-1} increase when Asp-150 is replaced with Glu or Asn. The intensities of these bands are larger in the D150E mutant than in the D150N mutant. On the other hand, the NR_K minus NR spectrum (shown with a dashed−dotted line) has much larger bands at 1394 (+)/1409 (−) cm^{-1}. Therefore, the observed spectral change of prolines is another similarity between the D150E mutant of LR and wild-type NR. According to the amino acid sequences of LR and NR, the proline residues which correspond to Pro-50 in BR are replaced with threonine, meaning that the bands come from Pro-145 and Pro-241 (LR numbering), which correspond to Pro-91 and Pro-186 of BR, respectively. The observed bands may come from Pro-145, because Asp-150, which is the substitution site, is located on the same helix. However, it should be noted that NR has another proline, Pro-264, at the position of Val-217 in BR, where LR has a glycine residue. One of the bands of NR observed in this frequency region may come from Pro-264.

Effect of the Replacement of Asp150 on the Hydrogen-Bonded Network in the Schiff Base Region Revealed by the O−D Stretches of Water and the N−D Stretches of the Schiff Base. In the past, we have characterized the hydrogen-bonded networks in the protein moiety of various rhodopsins through the analysis of the X−D stretching vibrations, which appear in the 2800−1800 cm^{-1} region (*13*, *16*, *35*−*38*). Because of strong infrared absorption of water, it is hard to observe the O−H and N−H stretching vibrations under strongly hydrogen bonded conditions when the sample is hydrated with H_2O. Therefore, it is better to split the spectrum into the X−H stretching region for the H−D nonexchangeable groups and the X−D stretching region for the exchangeable groups. Here, we concentrated on the X−D stretching region in investigating the hydrogen bonding of the internal water molecules and the retinal Schiff base.

In the higher-frequency region presented in Figure 6 (left panel), there are at least six bands that can be assigned to O−D stretching vibrations of water based on $D_2{}^{18}O$ isotope shifts (green labels). These bands downshift by 10−18 cm^{-1}

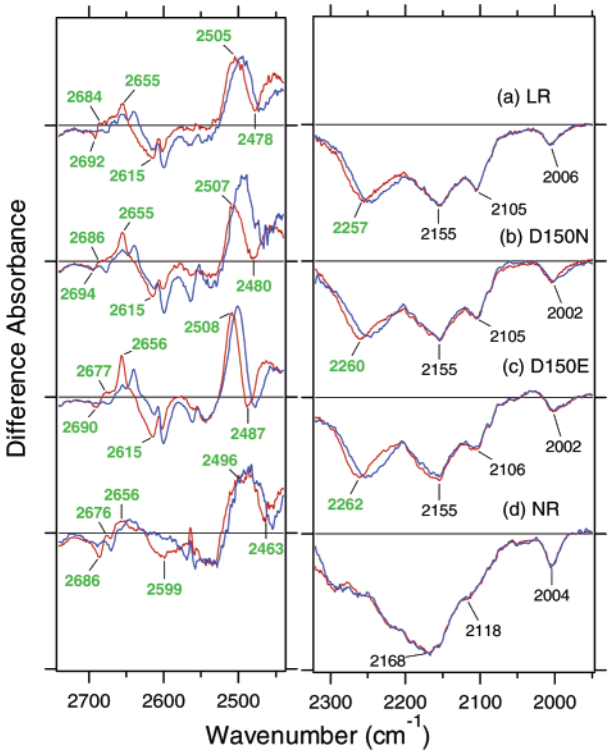

FIGURE 6: Difference infrared spectra between the K intermediates and the unphotolyzed states of wild-type (a), D150N (b), and D150E (c) LR and wild-type NR (d) in the 2740−2440 cm^{-1} region (left) and the 2320−1950 cm^{-1} region (right), where O−D stretching vibrations of water and N−D stretching vibrations of the Schiff base can be observed. The red and blue lines represent the spectra of samples measured under D_2O and $D_2{}^{18}O$ hydration, respectively. One division of the *y*-axis corresponds to 0.00054 (left) and 0.00045 (right) absorbance unit.

in the spectra measured with $D_2{}^{18}O$ hydration (blue lines) compared to the spectra measured with D_2O hydration (red lines), as shown in our previous reports (*13*, *16*). The water molecules with O−D stretches located at 2692, 2615, and 2478 cm^{-1} change their frequencies to 2684, 2655, and 2505 cm^{-1}, respectively, upon retinal isomerization in LR. In the case of BR, we recently assigned the water bands in the K minus BR spectrum to the water molecules found in the Schiff base region (*39*, *40*), corresponding to waters 401, 402, and 406 in the X-ray crystal structure (PDB entry 1C3W) (*25*). Judging from the sequence similarity, the water bands in LR and NR should also come from the water molecules around the Schiff base.

In this spectral range, the spectra of the D150N and D150E mutants of LR and wild-type NR are basically similar to that of wild-type LR. However, the relative intensities of two positive bands at 2655 and 2505 cm^{-1} increase in the D150N and, more evidently, D150E mutant. Such a phenomenon was not observed in the D96N mutant of BR (*40*). In addition, there is no positive band in the corresponding O−H stretching frequency region of the K_L minus BR spectra (*32*). Therefore, the bands at 2655 and 2505 cm^{-1} are characteristic of the K intermediate of LR and probably can be assigned to the same source as the bands at 2656 and 2496 cm^{-1} in the K intermediate of NR, but the location of these water molecules is not clear at present. The increase in the intensities of the bands may suggest that the hydrogen bond to the oxygen atom of the water molecule becomes stronger in the K intermediates of these mutants, resulting

in the increase in the level of electronic polarization of the O−H groups. Such phenomena were not observed in wild-type LR and NR, so the result indicates the specificity of the mutants.

In the lower-frequency region, strongly hydrogen bonded X−D groups can be observed as shown in the right panel of Figure 6. The negative bands at 2257, 2260, and 2262 cm^{-1} downshift in the spectra measured with $D_2{}^{18}O$ hydration, which indicates that these bands originate from water O−D stretches. Such a band is not seen in the spectrum of NR (Figure 6d). These results are related to our recently established empirical law stating that archaeal rhodopsins which exhibit proton pumping activity have strongly hydrogen bonded water in the Schiff base region. We believe that such a water molecule is essential for proton pumping. In the case of the studied LR mutants, the strongly hydrogen bonded water bands are present. Therefore, the primary proton pumping machinery is probably kept intact in these mutants, whereas the reprotonation rate of the Schiff base is dramatically reduced. The slight upshift of the water bands in the mutants (3 cm^{-1} in D150N and 5 cm^{-1} in D150E) may be caused by the change in interaction with Asp-139, which is the primary counterion of the protonated Schiff base and is located on the same helix as Asp-150 (helix C).

The negative bands at 2155 and 2105 cm^{-1} do not exhibit the isotope shift in $D_2{}^{18}O$ and could be assigned to the N−D stretching vibrations of the Schiff base on the basis of the analogy with other archaeal rhodopsins (*41*, *42*). These bands were not affected by the mutations of Asp150, similar to the case of the N−D in-plane and N−HOOP vibrations in the ground state of LR (Figure 3).

The K_L Intermediate of LR Resembles the Photoproduct of the D150 LR Mutants and Wild-Type NR at 77 K. The difference infrared spectra between the K_L intermediate and the ground state of LR are shown in Figure 7. The vibrational bands indicated by the tags are characteristic of the K_L intermediate except for the negative band at 1245 cm^{-1}, which is assigned to the ground state of LR and appears upon formation of the K_L, but not K, intermediate. The bands at 1355 and 1300 cm^{-1} can be assigned to the N−H in-plane vibrations as in the case of BR, the bands of which appeared at 1348 and 1294 cm^{-1} (*32*). The band at 981 cm^{-1} can be assigned to the C15−HOOP vibration like the band of the K_L intermediate of BR at 985 cm^{-1} (*32*). The difference spectra of the K intermediate of the D150 mutants, especially D150E, exhibit amplitude increases for the bands characteristic of the K_L intermediate. Interestingly, the spectrum of the K intermediate of NR is quite similar to that of the K_L intermediate of LR (Figure 7d). It is possible that the stabilities of the K intermediates of the D150E mutant of LR and wild-type NR are reduced and their K_L intermediates appear even at 77 K to some extent.

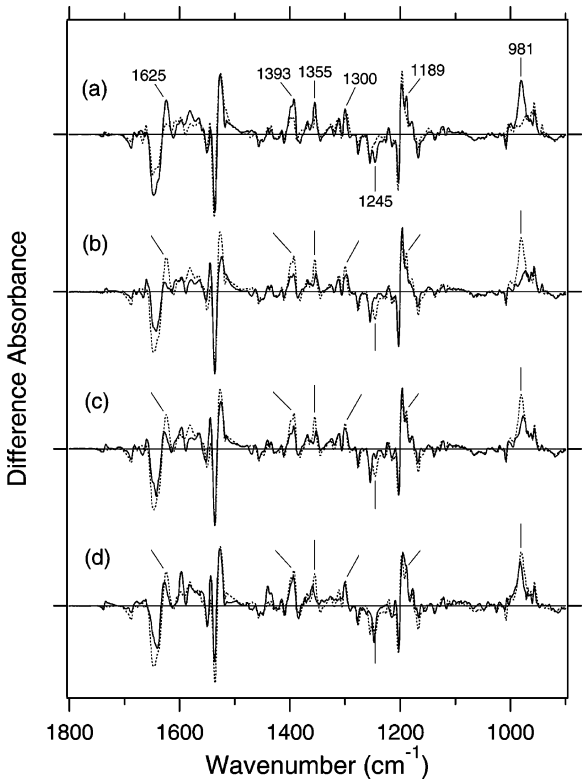

FIGURE 7: Comparison of the infrared spectra of the K_L intermediate of LR, trapped at 130 K, with those of the K intermediate of wild-type (a), D150N (b), and D150E (c) LR and wild-type NR (d) in the 1800−900 cm^{-1} region. The spectra were measured under H_2O hydration. The dotted lines in panels b−d are reproduced from the solid line in panel a, while the dotted line in panel a and the solid lines in panels b−d are reproduced from the spectra shown in Figure 2. The tags indicate the bands characteristic of the difference infrared spectrum of the K_L intermediate of LR. One division of the *y*-axis corresponds to 0.007 absorbance unit.

DISCUSSION

One of the contentious questions in the rhodopsin field, which became pressing lately due to the dramatic increase in the availability of the new protein sequences, is whether functions of new rhodopsins can be rationalized from their primary structures. In particular, it was believed that functions of microbial rhodopsins can be determined from the nature of the cytoplasmic residue corresponding to Asp-96 in BR, which serves as a proton donor for the Schiff base. Indeed, in haloarchaeal and eubacterial proton pumps, this residue is either Asp or Glu, while it is an aromatic residue in halobacterial sensory rhodopsins (*4*). This empirical rule does not seem to hold for eukaryotic microbial rhodopsins, where examples of nontransporting proteins with a carboxylic residue at this position are found in both fungi (*Neurospora*, NR) and algae (*Guillardia*) (*12*, *43*). The recent discovery of a proton pumping activity of another fungal rhodopsin (from *Leptosphaeria*, LR) (*5*, *15*) created a more pointed question of how two proteins as structurally similar as NR and LR can have such different photochemical and ion transporting properties (*1*). Both NR and LR conserve most of the residues important for proton transport in BR and have a carboxylic acid at the position of the cytoplasmic proton donor, but it is represented by Glu in NR and by Asp in LR. In this paper, we investigate whether this subtle difference in the structure of the carboxylic side chain may be responsible for the dramatic differences in the photochemical behavior (and, ultimately, the functional diversification) of NR and LR. To accomplish that, we used spectroscopic characterization of two LR mutants at position 150 (homologous to Asp-96 of BR), in which we either removed the carboxylic group or made it NR-like by the Glu → Asp substitution.

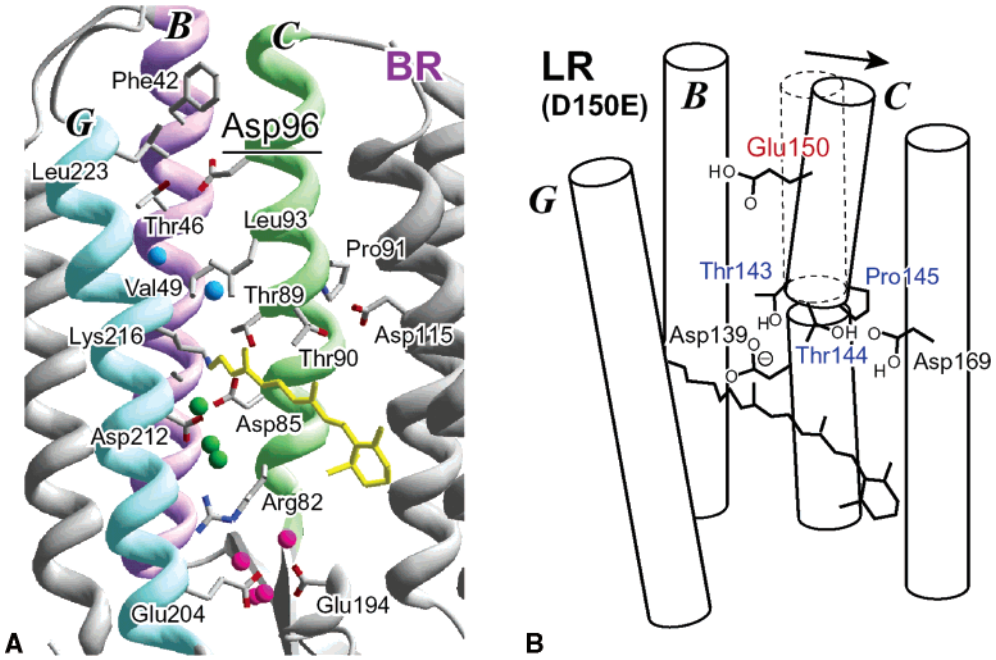

FIGURE 8: (A) X-ray crystal structure of BR (drawn from PDB entry 1C3W). The labeled amino acid residues in helices B, C, and G constitute the proton pathway and are conserved in LR and NR. The spheres represent the internal water molecules (colored according to location; blue for the intracellular side, green for the Schiff base region, and pink for the extracellular side). The water molecules colored green were called waters 401, 402, and 406 in the X-ray crystal structure (*25*). (B) Schematic representation of a possible structural alteration caused by the D150E mutation in LR. The arrangement of the helices is based on the crystal structure of BR presented in the left panel. We propose that the tilt of helix C at the kink at Pro-145 (Pro-91 in BR) may perturb the hydrogen bonds of Asp-139 and Thr-143 (Asp-85 and Thr-89 in BR, respectively) and Thr-144 and Asp-169 (Thr-90 and Asp-115 in BR, respectively).

We demonstrated that the replacement of the Schiff base proton donor Asp-150 with Glu severely impairs the reprotonation of the Schiff base of LR. Using flash photolysis of the LR D150E and D150N mutants heterologously expressed in *P. pastoris*, we found that the glutamic acid residue at this position is inefficient as a cytoplasmic proton donor (Figure 1), being functionally equivalent to a nonprotonatable asparagine. Such slow pH-dependent kinetics of Schiff base reprotonation is reminiscent of that for NR, where Glu-142 was found to be inactive as a proton donor (*12*). This is a surprising result, considering that Glu at this position functions as a proton donor in proteorhodopsin (*18*) as well as in *Escherichia coli*-expressed BR (*19*, *20*). On the other hand, there is a report that in the purple membrane this substitution decelerates reprotonation of the Schiff base dramatically (*21*). One of the simplest interpretations of this result would be that Glu-150 is deprotonated in the ground state and cannot work as a proton donor for the Schiff base. However, this explanation is invalidated by our FT-IR results showing that the C=O stretching vibration of the protonated carboxylic group of Glu-150 appears at 1718 cm^{-1}. Therefore, the phenotype should be explained from the structural point of view.

We applied low-temperature FT-IR in analyzing perturbations of the molecular structure of LR induced by the introduction of Glu or Asn at position 150. Asp-150 is homologous to Asp-96 in BR, which is located 12 Å from the retinal Schiff base nitrogen, suggesting that the structure around the Schiff base should not be changed by these mutations. Thus, it is remarkable that the LR_K minus LR difference spectra of the mutants, especially D150E, become more similar to that of NR (Figures 2−6), which has glutamate at the corresponding position. From our FT-IR results, the alteration of amide I vibrations (Figure 4) suggests that the packing of helices B, C, and G is affected by the mutations. The bands observed in the C−N stretching region of proline (Figure 5) suggest that the structural change of one of the proline residues may become larger than that of wild-type LR and similar to that of NR. One possible interpretation is that helix C may tilt at the flexible kink at Pro-145 (Pro-91 in BR) as a result of the side chain elongation or modification at position 150. Because Pro-50 on helix B in BR is replaced with threonine in LR and NR, the flexibility of helix B is probably reduced. Thus, it is a plausible assumption that the structural perturbation of helix B is smaller than that of helix C. This structural hypothesis is illustrated in Figure 8 (right panel). Such structural change would cause a perturbation of the hydrogen bonds between Thr-143 and Asp-139 (Thr-89 and Asp-85 in BR, respectively) and between Thr-144 and Asp-169 (Thr-90 and Asp-115 in BR, respectively). These effects are confirmed by the observed changes in the vibrational bands of Asp-169 and the water molecule bridging Asp-139 and the Schiff base nitrogen (Figures 4 and 6). However, most interestingly, as follows from the frequencies of the retinal C15−HOOP vibrations (Figure 3), the isomerization-induced torsion of the retinal near the Schiff base of the D150E mutant of LR is similar to that of NR. This structural view is also supported by the recently determined X-ray crystal structure of the D96A mutant of BR (*44*).[2]

[2] After the submission of our manuscript, the X-ray crystal structures of the D96A and T46V mutants of BR were published, which show that the distance between helices B and C increases and the hydrogen-bonded network around the Schiff base region is perturbed through the long-range interactions, especially in the D96A mutant.

The latter results on the similarity of the C15−HOOP vibrations of the primary photointermediates of the studied LR mutants to that of NR_K (Figure 3) require further comment. Previously, these vibrations were found to be similar for LR and BR but very different from those in NR and *p*pR (*16*), implying that the exact structure of the photoisomerized retinal may be important functionally. The dramatic change in the HOOP bands observed upon replacement of Asp-150 suggests that the conformation of the retinal can be controlled from this site, as previosuly shown for the Asp-96 mutants of BR (*45*). It should be noted that LR and NR have almost the same retinal binding site as shown in Figure 1 in ref *16*. There are 25 amino acid residues located within 5 Å of the retinal chromophore (if modeled on the basis of the BR structure). Among them, only one amino acid residue, Ala-196, which corresponds to Ser-141 in BR, is replaced with glycine in NR, a relatively conservative replacement. Therefore, the difference in the configuration of the photoisomerized retinal detected via the HOOP vibrations should not originate from the differences in the surrounding amino acids. Our results for the mutants of LR suggest that the long-range interactions, probably through the perturbation of helix C, can explain the differences in the C15−HOOP vibrations. A similar observation was made for the *p*pR mutant which has the same retinal binding site as BR (*46*), where the HOOP vibrations were observed at 982 and 959 cm^{-1} and exhibited spectral features between those of *p*pR and BR. This may be similar to the situation of the D150N mutant of LR, as *p*pR has a bulky amino acid, phenylalanine, at the corresponding site (Asp-96 of BR). Therefore, it is possible that the major reason for the defective retinal Schiff base reprotonation both in the mutant LR and in wild-type NR is the structural rearrangement through the conformational coupling between the cytoplasmic carboxylic acid and the retinal.

It should be noted that the upshift of the C15−HOOP vibration has been reported for the K_L intermediate of BR trapped at 135 K. A similar result was observed in LR as well. Therefore, it is reasonable to consider that the stability of K intermediates of the D150 mutants is reduced and the K_L intermediates are produced even at 77 K. The rearrangement of the helices may explain the lower stability of the K intermediate of the mutants. Namely, the tilt of helix C may allow a greater motional freedom of the retinal and facilitate the formation of the K_L intermediate at lower temperatures. Such motional freedom may be provided by the structural rearrangement around the Schiff base suggested by the X-ray crystal structure of the D96A mutant of BR (*44*).

The idea that the described glutamate for aspartate substitution can be a major structural determinant of the photochemistry and the functional diversification of fungal rhodopsins finds some support from the bioinformatic analysis. Normally, the LR-like proteins possess Asp at the position of the cytoplasmic proton donor, while the NR-like proteins contain Glu (*1*). Interestingly, the sequence of a gene encoding rhodopsin from *Chaetomium globosum*, very similar to that of NR otherwise, encodes Asn at the position homologous to position 142 of NR (position 150 of LR). This suggests that once the original aspartic proton donor is changed to glutamate, it becomes nonfunctional and can be replaced with a nonprotonatable residue with little or no change in functionality.

ACKNOWLEDGMENT

We thank Doreen E. Culham and Janet M. Wood for assistance in mutating the *ops* gene.

REFERENCES

1. Brown, L. S., and Jung, K. H. (2006) Bacteriorhodopsin-like proteins of eubacteria and fungi: The extent of conservation of the haloarchaeal proton-pumping mechanism, *Photochem. Photobiol. Sci. 5*, 538−546.
2. Ruiz-Gonzalez, M. X., and Marin, I. (2004) New insights into the evolutionary history of type 1 rhodopsins, *J. Mol. Evol. 58*, 348−358.
3. Spudich, J. L., and Jung, K. H. (2005) Microbial Rhodopsins: Phylogenetic and Functional Diversity, in *Handbook of Photosensory Receptors* (Briggs, W. R., and Spudich, J. L., Eds.) Wiley-VCH Verlag GmbH & Co. KGaA, Weinheim, Germany.
4. Spudich, J. L., Yang, C. S., Jung, K. H., and Spudich, E. N. (2000) Retinylidene proteins: Structures and functions from archaea to humans, *Annu. Rev. Cell Dev. Biol. 16*, 365−392.
5. Idnurm, A., and Howlett, B. J. (2001) Characterization of an opsin gene from the ascomycete *Leptosphaeria maculans*, *Genome 44*, 167−171.
6. Brown, L. S. (2004) Fungal rhodopsins and opsin-related proteins: Eukaryotic homologues of bacteriorhodopsin with unknown functions, *Photochem. Photobiol. Sci. 3*, 555−565.
7. Bieszke, J. A., Braun, E. L., Bean, L. E., Kang, S., Natvig, D. O., and Borkovich, K. A. (1999) The nop-1 gene of *Neurospora crassa* encodes a seven transmembrane helix retinal-binding protein homologous to archaeal rhodopsins, *Proc. Natl. Acad. Sci. U.S.A. 96*, 8034−8039.
8. Idnurm, A., and Heitman, J. (2005) Light controls growth and development via a conserved pathway in the fungal kingdom, *PLoS Biol. 3*, e95.
9. Prado, M. M., Prado-Cabrero, A., Fernandez-Martin, R., and Avalos, J. (2004) A gene of the opsin family in the carotenoid gene cluster of *Fusarium fujikuroi*, *Curr. Genet. 46*, 47−58.
10. Saranak, J., and Foster, K. W. (1997) Rhodopsin guides fungal phototaxis, *Nature 387*, 465−466.
11. Bieszke, J. A., Spudich, E. N., Scott, K. L., Borkovich, K. A., and Spudich, J. L. (1999) A eukaryotic protein, NOP-1, binds retinal to form an archaeal rhodopsin-like photochemically reactive pigment, *Biochemistry 38*, 14138−14145.
12. Brown, L. S., Dioumaev, A. K., Lanyi, J. K., Spudich, E. N., and Spudich, J. L. (2001) Photochemical reaction cycle and proton transfers in *Neurospora* rhodopsin, *J. Biol. Chem. 276*, 32495−32505.
13. Furutani, Y., Bezerra, A. G., Jr., Waschuk, S., Sumii, M., Brown, L. S., and Kandori, H. (2004) FTIR spectroscopy of the K photointermediate of *Neurospora rhodopsin*: Structural changes of the retinal, protein, and water molecules after photoisomerization, *Biochemistry 43*, 9636−9646.
14. Furutani, Y., Shibata, M., and Kandori, H. (2005) Strongly hydrogen-bonded water molecules in the Schiff base region of rhodopsins, *Photochem. Photobiol. Sci. 4*, 661−666.
15. Waschuk, S. A., Bezerra, A. G., Jr., Shi, L., and Brown, L. S. (2005) *Leptosphaeria* rhodopsin: Bacteriorhodopsin-like proton pump from a eukaryote, *Proc. Natl. Acad. Sci. U.S.A. 102*, 6879−6883.
16. Sumii, M., Furutani, Y., Waschuk, S. A., Brown, L. S., and Kandori, H. (2005) Strongly hydrogen-bonded water molecule present near the retinal chromophore of *Leptosphaeria* rhodopsin, the bacteriorhodopsin-like proton pump from a eukaryote, *Biochemistry 44*, 15159−15166.
17. Balashov, S. P., Imasheva, E. S., Ebrey, T. G., Chen, N., Menick, D. R., and Crouch, R. K. (1997) Glutamate-194 to cysteine mutation inhibits fast light-induced proton release in bacteriorhodopsin, *Biochemistry 36*, 8671−8676.
18. Dioumaev, A. K., Brown, L. S., Shih, J., Spudich, E. N., Spudich, J. L., and Lanyi, J. K. (2002) Proton transfers in the photochemical reaction cycle of proteorhodopsin, *Biochemistry 41*, 5348−5358.
19. Holz, M., Drachev, L. A., Mogi, T., Otto, H., Kaulen, A. D., Heyn, M. P., Skulachev, V. P., and Khorana, H. G. (1989) Replacement of aspartic acid-96 by asparagine in bacteriorhodopsin slows both the decay of the M intermediate and the associated proton movement, *Proc. Natl. Acad. Sci. U.S.A. 86*, 2167−2171.

20. Mogi, T., Stern, L. J., Marti, T., Chao, B. H., and Khorana, H. G. (1988) Aspartic acid substitutions affect proton translocation by bacteriorhodopsin, *Proc. Natl. Acad. Sci. U.S.A. 85*, 4148−4152.
21. Dyukova, T., Robertson, B., and Weetall, H. (1997) Optical and electrical characterization of bacteriorhodopsin films, *Biosystems 41*, 91−98.
22. Kandori, H., Shimono, K., Sudo, Y., Iwamoto, M., Shichida, Y., and Kamo, N. (2001) Structural changes of *pharaonis* phoborhodopsin upon photoisomerization of the retinal chromophore: Infrared spectral comparison with bacteriorhodopsin, *Biochemistry 40*, 9238−9246.
23. Kataoka, M., Kamikubo, H., Tokunaga, F., Brown, L. S., Yamazaki, Y., Maeda, A., Sheves, M., Needleman, R., and Lanyi, J. K. (1994) Energy coupling in an ion pump. The reprotonation switch of bacteriorhodopsin, *J. Mol. Biol. 243*, 621−638.
24. Tittor, J., Soell, C., Oesterhelt, D., Butt, H. J., and Bamberg, E. (1989) A defective proton pump, point-mutated bacteriorhodopsin Asp96 → Asn is fully reactivated by azide, *EMBO J. 8*, 3477−3482.
25. Luecke, H., Richter, H. T., and Lanyi, J. K. (1998) Proton transfer pathways in bacteriorhodopsin at 2.3 angstrom resolution, *Science 280*, 1934−1937.
26. Braiman, M., and Mathies, R. (1980) Resonance Raman evidence for an all-trans to 13-cis isomerization in the proton-pumping cycle of bacteriorhodopsin, *Biochemistry 19*, 5421−5428.
27. Furutani, Y., Sudo, Y., Wada, A., Ito, M., Shimono, K., Kamo, N., and Kandori, H. (2006) Assignment of the hydrogen-out-of-plane and in-plane vibrations of the retinal chromophore in the K intermediate of *pharaonis* phoborhodopsin, *Biochemistry 45*, 11836−11843.
28. Gat, Y., Grossjean, M., Pinevsky, I., Takei, H., Rothman, Z., Sigrist, H., Lewis, A., and Sheves, M. (1992) Participation of bacteriorhodopsin active-site lysine backbone in vibrations associated with retinal photochemistry, *Proc. Natl. Acad. Sci. U.S.A. 89*, 2434−2438.
29. Kukura, P., McCamant, D. W., Yoon, S., Wandschneider, D. B., and Mathies, R. A. (2005) Structural observation of the primary isomerization in vision with femtosecond-stimulated Raman, *Science 310*, 1006−1009.
30. Rothschild, K. J., and Marrero, H. (1982) Infrared evidence that the Schiff base of bacteriorhodopsin is protonated: bR570 and K intermediates, *Proc. Natl. Acad. Sci. U.S.A. 79*, 4045−4049.
31. Maeda, A., Sasaki, J., Pfefferle, J. M., Shichida, Y., and Yoshizawa, T. (1991) Fourier transform infrared spectral studies on the Schiff base mode of all-*trans* bacteriorhodopsin and its photointermediates, K and L, *Photochem. Photobiol. 54*, 911−921.
32. Maeda, A., Verhoeven, M. A., Lugtenburg, J., Gennis, R. B., Balashov, S. P., and Ebrey, T. G. (2004) Water Rearrangement around the Schiff Base in the Late K (K_L) Intermediate of the Bacteriorhodopsin Photocycle, *J. Phys. Chem. B 108*, 1096−1101.
33. Braiman, M. S., Mogi, T., Marti, T., Stern, L. J., Khorana, H. G., and Rothschild, K. J. (1988) Vibrational spectroscopy of bacteriorhodopsin mutants: Light-driven proton transport involves protonation changes of aspartic acid residues 85, 96, and 212, *Biochemistry 27*, 8516−8520.
34. Gerwert, K., Hess, B., and Engelhard, M. (1990) Proline residues undergo structural changes during proton pumping in bacteriorhodopsin, *FEBS Lett. 261*, 449−454.
35. Kandori, H., Kinoshita, N., Yamazaki, Y., Maeda, A., Shichida, Y., Needleman, R., Lanyi, J. K., Bizounok, M., Herzfeld, J., Raap, J., and Lugtenburg, J. (1999) Structural change of threonine 89 upon photoisomerization in bacteriorhodopsin as revealed by polarized FTIR spectroscopy, *Biochemistry 38*, 9676−9683.
36. Kandori, H., Kinoshita, N., Yamazaki, Y., Maeda, A., Shichida, Y., Needleman, R., Lanyi, J. K., Bizounok, M., Herzfeld, J., Raap, J., and Lugtenburg, J. (2000) Local and distant protein structural changes on photoisomerization of the retinal in bacteriorhodopsin, *Proc. Natl. Acad. Sci. U.S.A. 97*, 4643−4648.
37. Kandori, H., Yamazaki, Y., Shichida, Y., Raap, J., Lugtenburg, J., Belenky, M., and Herzfeld, J. (2001) Tight Asp-85−Thr-89 association during the pump switch of bacteriorhodopsin, *Proc. Natl. Acad. Sci. U.S.A. 98*, 1571−1576.
38. Kandori, H., Furutani, Y., Shimono, K., Shichida, Y., and Kamo, N. (2001) Internal water molecules of *pharaonis* phoborhodopsin studied by low-temperature infrared spectroscopy, *Biochemistry 40*, 15693−15698.
39. Shibata, M., Tanimoto, T., and Kandori, H. (2003) Water molecules in the Schiff base region of bacteriorhodopsin, *J. Am. Chem. Soc. 125*, 13312−13313.
40. Shibata, M., and Kandori, H. (2005) FTIR studies of internal water molecules in the Schiff base region of bacteriorhodopsin, *Biochemistry 44*, 7406−7413.
41. Shimono, K., Furutani, Y., Kamo, N., and Kandori, H. (2003) Vibrational modes of the protonated Schiff base in *pharaonis* phoborhodopsin, *Biochemistry 42*, 7801−7806.
42. Kandori, H., Belenky, M., and Herzfeld, J. (2002) Vibrational frequency and dipolar orientation of the protonated Schiff base in bacteriorhodopsin before and after photoisomerization, *Biochemistry 41*, 6026−6031.
43. Sineshchekov, O. A., Govorunova, E. G., Jung, K. H., Zauner, S., Maier, U. G., and Spudich, J. L. (2005) Rhodopsin-mediated photoreception in cryptophyte flagellates, *Biophys. J. 89*, 4310−4319.
44. Lanyi, J. K., and Schobert, B. (2006) Propagating structural perturbation inside bacteriorhodopsin: Crystal structures of the M state and the D96A and T46V mutants, *Biochemistry 45*, 12003−12010.
45. Dioumaev, A. K., Brown, L. S., Needleman, R., and Lanyi, J. K. (1998) Partitioning of free energy gain between the photoisomerized retinal and the protein in bacteriorhodopsin, *Biochemistry 37*, 9889−9893.
46. Shimono, K., Furutani, Y., Kandori, H., and Kamo, N. (2002) A *pharaonis* phoborhodopsin mutant with the same retinal binding site residues as in bacteriorhodopsin, *Biochemistry 41*, 6504−6509.

BI061864L